Pergamon

Bioorganic & Medicinal Chemistry 8 (2000) 1871–1880

BIOORGANIC & MEDICINAL CHEMISTRY

Synthesis of Fluorescent Microgonotropens (FMGTs) and Their Interactions with dsDNA

Alexander L. Satz and Thomas C. Bruice*

Department of Chemistry, University of California at Santa Barbara, Santa Barbara, CA 93106, USA

Received 21 January 2000; accepted 29 March 2000

Abstract—A new class of microgonotropen compounds (FMGTs), which fluoresce upon binding to dsDNA, is introduced. The FMGTs consist of a minor groove binding moiety based upon Hoescht 33258 covalently attached to a polyamine chain capable of interacting with the phosphodiester backbone of dsDNA. The interactions of FMGTs with dsDNA were investigated by fluorescence and UV spectroscopy. Several different dsDNA oligomers were studied to determine the effect of binding site sequence on stoichiometry and binding affinity. The FMGTs were found to bind a dsDNA oligomer that contained the sequence 5′-AATTT-3′ with FMGT:dsDNA stoichiometries equal to 2:1 or 3:1. Hoechst 33258 bound the same dsDNA oligomer with a 1:1 stoichiometry. The second and third order equilibrium constants for complexation were determined to be $\mathrm{Log}(K_1K_2) = 17.9\,\mathrm{M}^{-2}$ and $\mathrm{Log}(K_1K_2K_3) = 26.1\,\mathrm{M}^{-3}$, respectively, for two of strongest binding FMGTs. From thermal melting experiments ΔT_m for Hoechst 33258 was determined to be 10 °C while the ΔT_m values for FMGTs ranged from 20–26 °C indicating the greater stability of the latter.

Introduction

Reagents capable of sequence selective recognition of DNA, particularly small organic compounds capable of binding to the minor groove of B-DNA, have drawn tremendous attention due to their known biological activity and diverse medicinal uses.[1–12] Recent in vitro studies indicate that these agents may influence the regulation of gene expression since they have been shown to inhibit the binding of regulatory proteins to their DNA consensus binding sites.[13–21] These same studies indicate that the inhibitory activity of often studied minor groove binders as distamycin, netropsin, Hoechst 33258, etc., are rather limited to proteins which reside within the minor groove. Detrimental to the potential ability of the above mentioned minor groove binders to specifically inhibit protein binding is their lack of interaction with DNA outside the minor groove coupled with minimal distortion of the DNA helix upon complexation.[22–24]

We have investigated a novel class of minor groove binding ligands, microgonotropens (MGTs), which consist of an A/T-selective DNA minor groove binding tripyrrole peptide and polyamine chains attached to the central pyrrole that interact electrostatically with the phosphodiester backbone of dsDNA (Fig. 1).[13,16,25,26] MGTs were shown to be extraordinarily effective inhibitors of the association of the transcription factor E2 factor 1 (E2F1), to its DNA promoter element.[15] The most active MGT, MGT-6a, was three orders of magnitude more effective than distamycin.

We now report studies of a minor groove binding moiety based upon the widely used DNA fluorophore Hoechst 33258, known to bind A/T rich sequences of dsDNA.[25–32] Hoechst 33258's increase in fluorescence emission intensity upon binding dsDNA allows for expeditious determination of ligand:dsDNA binding stoichiometry and equilibrium constants for complexation.[26,32,33]

Results and Discussion

Synthesis

FMGTs were sythesized with a *meta* linker arm to direct the polyamine moiety out of the minor groove (Scheme 1).[8,9,34] The choice of 4-hydroxybutyrate as the linker arm for the FMGTs was based upon its relative flexibility, length, and synthetic accessibility. Termination of the linker arm with a carboxylic acid allows for coupling to a polyamine chain using solution or solid-phase chemistry. Polyamine chains were chosen based upon synthetic accessibility and the results previously shown by the tripyrrole peptide MGTs.[35]

*Corresponding author. Tel.: +1-805-961-2044; fax: +1-805-893-4120; e-mail: tcbruice@bioorganic.ucsb.edu

0968-0896/00/$ - see front matter
PII: S0968-0896(00)00116-4

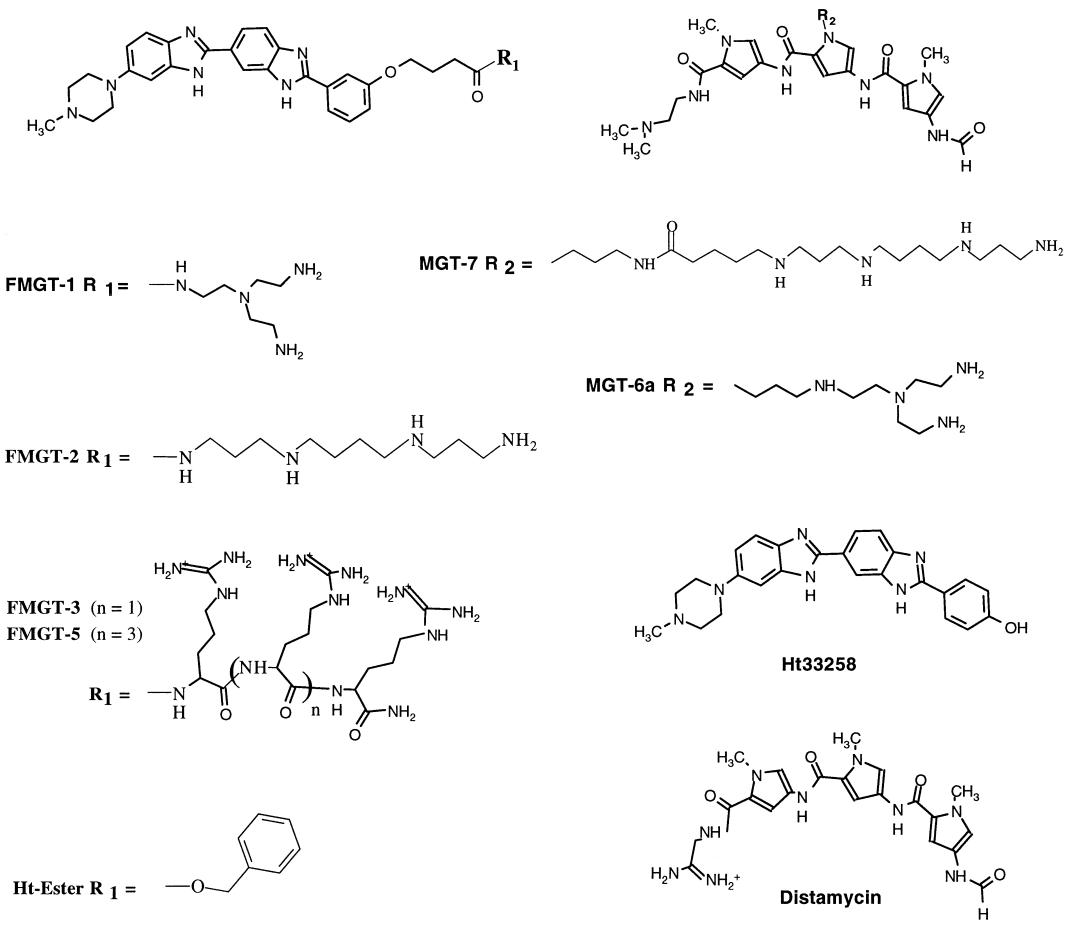

Figure 1. The structures of FMGT-1, -2, -3, and -5, Ht-Ester, tripyrrole peptide MGT-7, and -6a, Hoechst 33258, and distamycin.

Mitsunobu[36] type reaction of 3-hydroxybenzaldehyde (**1**) with 4-hydroxybutyrate[37] gave **2**. Condensation of the appropriate *ortho* diamine with **2** gave **3**.[38] Deprotection of the carboxylic acid derivative by base hydrolysis yielded **4**. PyBOP®[39] was used for all peptide coupling reactions. Synthesis of FMGTs-3 and -5 were accomplished using standard solid-phase FMOC techniques. PyBOP® coupling reactions of **4** to the terminal amine of the polyarginine chain (3 or 5 peptides long) where achieved in DMF using a 2-fold excess of **4**.

Thermal melting experiments and fluorescence spectroscopy

Table 1 lists the thermal melting temperatures of dsDNAs **20** and **21** when complexed with FMGTs (see Table 1 for dsDNA sequences and Fig. 2 for thermal melting curves). The dsDNA sequence **21** is a shortened variation of the 27 base pair derivative of the hamster dihydrofolate reductase promoter which was the dsDNA sequence used to determine the E2F1 inhibitory activity of tripyrrole peptide MGTs.[15] The dsDNA **20** is a derivative of **21** that lacks an A/T rich sequence and was used as the control in this study.

Thermal melting experiments gave a ΔT_m for Hoechst 33258:**21** of 10 °C while ΔT_m values for the FMGT:**21** complexes ranged from 20–26 °C. FMGT-2 formed the most stable dsDNA complex with a ΔT_m of 26 °C, roughly 2.5 times larger than that for Hoechst 33258. Experiments using the control sequence **20** indicate substantial duplex stabilization by the FMGTs although ΔT_m values for FMGT:**21** complexes are still significantly greater. The ΔT_m values for the FMGT:**20** complexes ranged from 11 to 19 °C.

Measurement of fluorescence intensity upon titration of an appropriately large concentration of dsDNA with Hoechst 33258 provides an essentially linear relationship between emission intensity and Hoechst 33258 concentration up to the point of binding site saturation. The molar ratio (stoichiometry) of ligand to dsDNA is determined by measuring the point of intersection of the two slopes of the titration (Fig. 3). The stoichiometries for Hoechst 33258:**21** and FMGT:**21** complexes were determined to be 1:1 for Hoechst 33258, 2:1 for FMGT-1, and -3, and 3:1 for FMGT-2, and -5. Attempts to determine the stoichiometries of the Hoechst 33258 and FMGT-1:**20** complexes were made due to the 13 °C ΔT_m value of the latter, however the ligand:**20** complexes were found to not be fluorescent. Thermal melting experiments and fluorescence spectroscopy provide little insight into the nature of the FMGT:**20** complexes. Some possibilities include DNA intercalation and/or minor groove binding with altered sequence selectivity. Both of these alternative types of DNA binding have

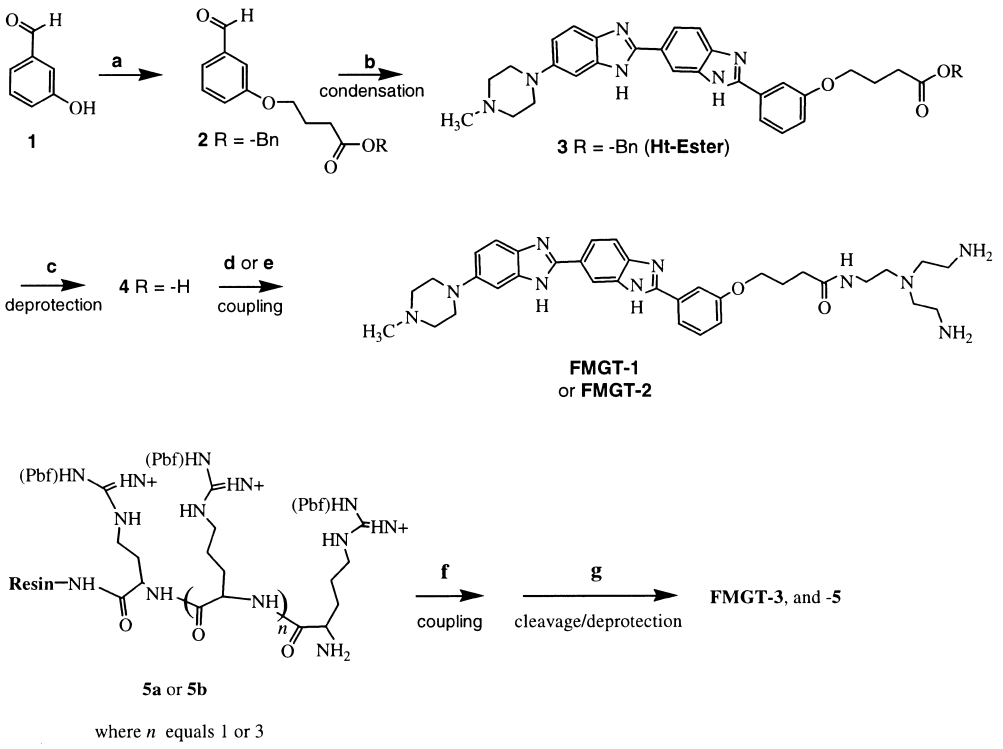

Scheme 1. (a) 4-Hydroxybutyrate, $(Ph)_3P$, DEAD, DCM; (b) 2-(3,4-Diaminophenyl)-6-(4-methyl-1-piperazinyl)benzimidazole, nitrobenzene, 120 °C; (c) K_2CO_3, DMF, H_2O, 90 °C; (d) PyBOP®, tris(2-aminoethyl)amine, DMF; (e) PyBOP®, spermine, DMF; (f) PyBOP®, **4**, DMF; (g) 95% TFA, 2.5% triisopropylsilane, 2.5% water. Pbf = 2,2,4,6,7-pentamethyldihydrobenzofuran-5-sulfonyl.

Table 1. Thermal melting temperatures (°C) for dsDNA **20** and **21**[a,b]

	20	**21**
No ligand	57	55
Hoechst 33258	60	65
FMGT-1	70	77
FMGT-2	76	81
FMGT-3	68	76
FMGT-5	68	77

[a]Melting points were determined by first derivative analysis.
[b]The dsDNA oligomers d(GCGACTGCAATTTCGACGTCC) and d(CGACGACTGCAACGACGTCC) and are referred to as **21** and **20**, respectively.

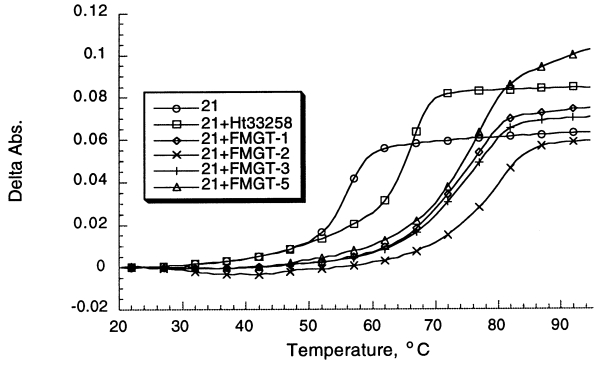

Figure 2. Thermal melting curves for dsDNA:ligand complexes. Absorbance measurements were taken every 1°C (for clarity only one in five data points are represented by a symbol). 0.80 μM dsDNA **21**, 2.8 μM ligand when present.

been shown to occur with either Hoechst 33258 or related analogues.[40–43]

Table 2 provides the relative molar fluorescence emission intensities of Hoechst 33258 and the FMGTs as measured at the wavelength of maximum signal intensity, λ_{max}, when excited at 354 nm (fluorescence intensities for the unbound fluorophores do not increase linearly with increasing concentrations, especially at higher, μM, concentrations). The λ_{max} was found to be approximately 480 nm for all unbound ligands and 470 nm for all ligands when bound to dsDNA except Hoechst 33258 whose λ_{max} blue shifts roughly 30 to 450 nm when bound.

Compared to Hoechst 33258 the FMGTs show a weaker fluorescence signal and less of a blue shift in λ_{max} upon forming a ligand:**21** complex. It is believed that fluorophores such as Hoechst 33258 fluorescence weakly in aqueous solution due to quenching by water and that complexation within the minor groove of dsDNA limits water accessibility and a corresponding increase in quantum yield results. As mentioned by a reviewer, it is tempting to argue that the quantum yield of fluorescence correlates with tighter or 'deeper' binding (this idea has been previously raised by Robles and McLaughlin, ref 44) and that the lower quantum yield for the FMGTs results from weaker or 'less deep' binding within the minor groove. Of course, this conclusion can only be valid if Hoechst 33258 and the FMGTs have equal quantum yields underneath the same conditions. By taking the fluorescence spectra of Hoechst 33258 and FMGT-1 in methanol the two molecules were shown to not be spectroscopically identical. The solvent methanol was chosen because unlike in water

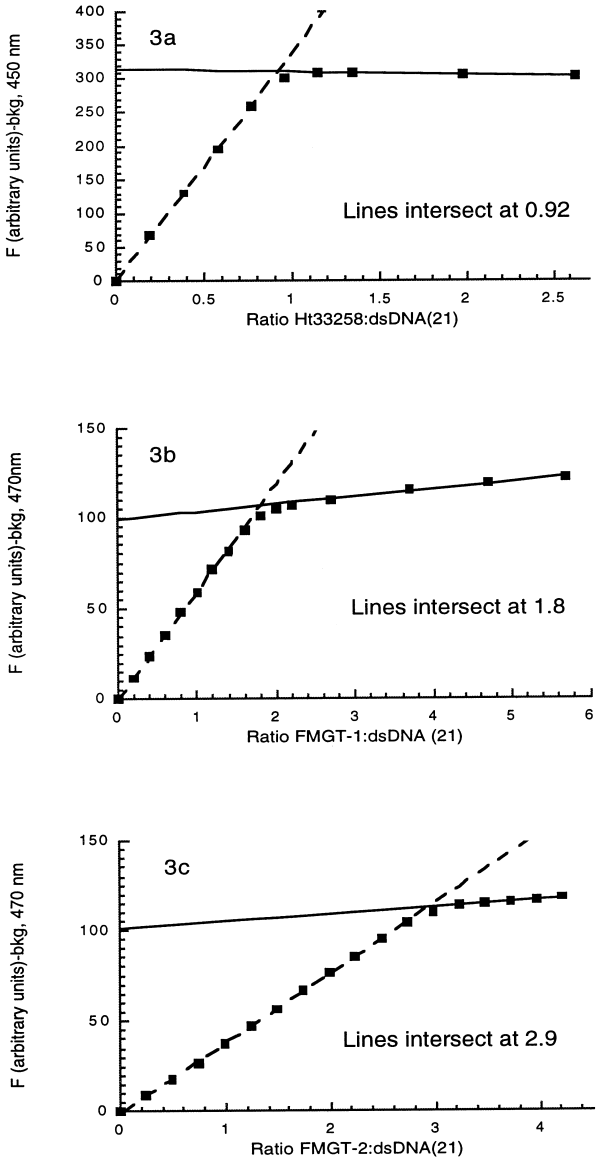

Figure 3. Representative fluorescent titrations of a constant concentration of dsDNA, 50 μM, with ligand for determination of ligand:**21** stoichiometries. Samples were excited at 354 nM and their fluorescence emission scanned between 400 and 500 nM. Plots shown are of signal intensity subtracted by background intensity. (a) Titration with Hoechst 33258. (b) Titration with FMGT-1. (c) Titration with FMGT-2.

the fluorophores give a strong signal. The results in Table 2 show that the structural differences between Hoechst 33258 and FMGT-1 significantly affect their fluorescence spectra in both quantum yield and λ_{max}.

Determination of binding constants[33]

For cases in which binding stoichiometries were 1:1, association constants were calculated by curve fitting analysis of the isothermal binding curves using either eqs (1) and (2) or eqs (1) and (4). Equations (1) and (2) can be used to fit the plots of fluorescence versus total concentration of ligand ($[L]_T$) added to a constant concentration of dsDNA. Alternatively, the expression of eq. (1) can be employed to fit plots of fluorescence versus concentration of unbound ligand ($[L]_f$). Where $[L]_f$ is calculated by eq (4). eq (4) is derived from eq (3). For 2:1 or 3:1 binding, the mathematical solution for $[L]_f$ is more complex than the quadratic solution given in eq (2). Plots of fluorescence versus $[L]_f$ are used to calculate the equilibrium constants by curve fitting with eqs (5) or (6) for 2:1 or 3:1, respectively. The derivation and use of eq (5) has been discussed by our laboratory.[26]

Table 2. Fluorescence emission of ligand and ligand: **21** complexes

	F(intensity) unbound ligand[a]	*F*(intensity) ligand:**21**$_x$ complexes[b]
Hoechst 33258	96	6200
FMGT-1	10	2400
FMGT-2	80	2300
FMGT-3	51	4000
FMGT-5	36	2600
Ht-Ester	27	3500
Hoechst 33258 in methanol	7200 (λ_{max} = 466 nM)	
FMGT-1 in methanol	520 (λ_{max} = 480 nM)	

[a]Fluorescence (arbitrary units), adjusted to μM^{-1} ligand, determined at λ_{max} as given in the text. All measurement made in buffered, pH 7.2, aqueous solution except for the last two entries in which methanol was used as the solvent.
[b]Fluorescence (arbitrary units), adjusted to μM^{-1} complex dsDNA: ligand$_x$, where x describes the stoichiometry of binding as given in the text.

$$F = \sum \Phi_f \left(\frac{K[L]_f}{1 + K[L]_f} \right) \quad (1)$$

where $\Sigma\Phi_f$ is the total fluorescence intensity upon saturation of dsDNA binding sites with ligand, K is the equilibrium constant, and $[L]_f$ is the concentration of ligand free in solution.

$$[L]_f = 0.5\left(-b + \sqrt{b^2 + \frac{4[L]_T}{K}} \right) \quad (2)$$

where $b = [\mathrm{DNA}]_\mathrm{T} - [L]_T + 1/\mathrm{K}$ and $[\mathrm{DNA}]_\mathrm{T}$ is the total concentration of dsDNA in the sample.

$$F = \sum \Phi_f \frac{[L]_{\mathrm{Bound}}}{n[\mathrm{DNA}]_\mathrm{T}} \quad (3)$$

where $[L]_{\mathrm{Bound}}$ is the concentration of ligand bound to dsDNA, and n is the stoichiometry of binding.

$$[L]_f = [L]_T - \frac{n[\mathrm{DNA}]_\mathrm{T} F}{\sum \Phi_f} \quad (4)$$

$$F = \sum \Phi_f \left(\frac{0.5K_1[L]_f + K_1K_2[L]_f^2}{1 + K_1[L]_f + K_1K_2[L]_f^2} \right) \quad (5)$$

$$F = \sum \Phi_f \left(\frac{1/3K_1[L]_f + 2/3K_1K_2[L]_f^2 + K_1K_2K_3[L]_f^3}{1 + K_1[L]_f + K_1K_2[L]_f^2 + K_1K_2K_3[l]_f^3} \right) \quad (6)$$

Table 3 lists the calculated equilibrium constants for complexation for FMGTs with **21** as determined by curve fitting using the appropriate theoretical model. The combined equilibrium constants $Log(K_1K_2)$ for 2:1 binding, or $Log(K_1K_2K_3)$ for 3:1 binding, are reported since separation of the individual equilibrium constants was not possible. Figure 3 shows representative isothermal binding curves and their fits. The combined equilibrium constants for complexation of **21** by FMGT-1 (K_1K_2) is roughly an order of magnitude larger than FMGT-3's and two orders of magnitude larger than Hoechst Ester's. The binding curves for FMGT-3 and Hoechst Ester show an 'S' shape by visual inspection, an indication of cooperative binding presumably as a dimer. FMGT-1 also shows an 'S' shaped binding curve although less pronounced than for FMGT-3 and Hoechst Ester. The cooperative binding of Hoechst Ester shows that the polyamine chain is not the cause of the higher order binding. The multiplied through equilibrium constants for complexation of **21** by FMGT-2 ($K_1K_2K_3$) is two orders of magnitude larger than that of FMGT-5's. As for the 2:1 binders, FMGT-2 and -5 both have an 'S' shaped binding curve, although it is more noticeable for FMGT-2 (Fig. 4b). In the determination of equilibrium constants of complexation it was assumed that complexation of **21** outside of the A/T rich site had no significant effect on the observed fluorescent signal since ligand:**20** complexes do not fluoresce and their complexes are less stable than those with **21**.

It is likely that higher order binding by FMGTs occur solely within the A/T rich sequence of **21** in a cooperative manner as a dimer or trimer. The effect of binding site size on equilibrium constant for complexation was investigated using dsDNA **20b** d(GGACGTCGAATTGCAGTCGC) which contains a binding site of four contiguous base pairs compared to five for **21**. It was assumed that monomeric, dimeric, and trimeric binding modes would be affected differently by a reduction in size of the A/T rich sequence. The oligomer **20b** was titrated with either Hoechst 33258, FMGT-1, or FMGT-2 whose complexes with **21** had stoichiometries of 1:1, 2:1, and 3:1, respectively.

The equilibrium constant for Hoechst 33258 changes little between **21** and **20b**. The K_1K_2 term for FMGT-1 is an order of magnitude less for **20b** than for **21**. The $K_1K_2K_3$ term for FMGT-2 decreases by two orders of magnitude when complexed with **20b**. The decreases in the combined equilibrium constants for complexation of the FMGTs is difficult to explain without assuming that complexation occurs solely within the A/T rich sequence.

Table 3. Combined equilibrium constants for complexation between FMGTs and dsDNA oligomers **20b** and **21**[a]

Ligand	Equilibrium constants for complexation with **20b**[b]	Equilibrium constants for complexation with **21**[c]
Ht33258	$Log(K_1) = 9.2\,M^{-1}$	$Log(K_1) = 9.6\pm0.3\,M^{-1}$
FMGT-1	$Log(K_1K_2) = 16.6\,M^{-2}$	$Log(K_1K_2) = 17.9\pm0.1\,M^{-2}$
FMGT-2	$Log(K_1K_2K_3) = 23.7\,M^{-3}$	$Log(K_1K_2K_3) = 26.1\pm0.4\,M^{-3}$
FMGT-3		$Log(K_1K_2) = 17.0\pm0.1\,M^{-2}$
FMGT-5		$Log(K_1K_2K_3) = 23.6\pm0.4\,M^{-3}$
Ht-Ester		$Log(K_1K_2) = 15.8\,M^{-2}$ [b]

[a]Determined by nonlinear least squares fitting of an isothermal binding curve with the appropriate theoretical model. Equilibrium constants are given as $Log(K_1)$, $Log(K_1K_2)$, or $Log(K_1K_2K_3)$ for 1:1, 2:1, or 3:1 binding stoichiometries respectively since separation of the individual equilibrium constants was not possible. **21** = d(GCGACTGCAATTTCGACGTCC) and **20b** = d(GGACGTCGAATTGCAGTCGC).

[b]The combined equilibrium constants were determined from a single isothermal titration.

[c]Combined equilibrium constants were calculated as the average of at least three trials. Error values were derived from the standard deviations between trials.

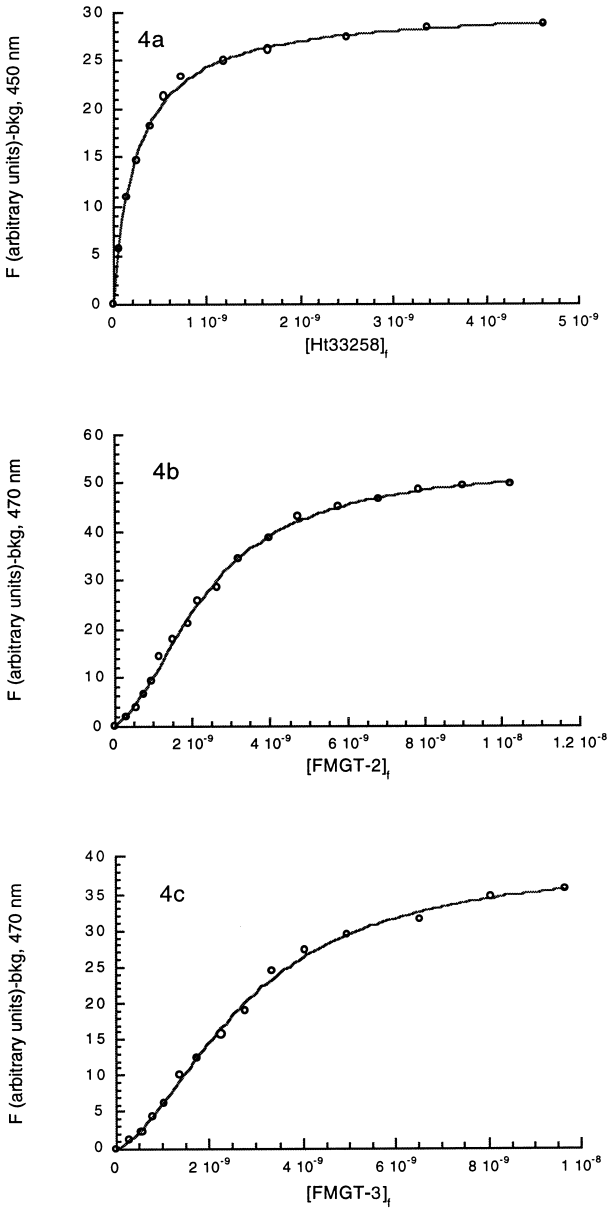

Figure 4. Isothermal binding curves generated by fluorescent titrations of a constant concentration of dsDNA with ligand. Samples, 1–5 nM **21**, were titrated with concentrated (μM) ligand solutions. Samples were excited at 354 nm and their fluorescence emission monitored at the appropriate wavelength. Fluorescence intensities have been subtracted by the background value. The x-axis gives the concentration of unbound ligand $[L]_f$ as calculated by eq (4) (see text). Data points are then fit using the theoretical model described by eqs (1), (5), or (6) and a nonlinear least squares curve fitting routine. (a) 1 nM **21** titrated with Hoechst 33258. (b) 2 nM **21** titrated with FMGT-2. (c) 1 nM **21** titrated with FMGT-3.

Then it can be concluded that the monomer, dimer, and trimer are successsively more sensitive to binding site size. The 3:1 binding reported here, if it is occurring within a single binding site, is certainly not usual. To this time the only report of greater than a 2:1 stoichiometry for any minor groove binder has been by Blasko and Bruice[45] who reported the binding of distamycin to dsDNA in a 4:1 stoichiometry.

The dsDNA **12** d(CCGGAATTCCGG) also contains an A/T rich binding site of 4 base pairs. The equilibrium constants for complexation of Hoechst 33258 with dsDNA **12** has been previously published and is within an order of magnitude of the value obtained in this laboratory of $\text{Log}(K_1) = 9.1\ \text{M}^{-1}$.[46] This value differs little from the values obtained for the oligomers **20b** or **21** as given in Table 3. Surprisingly, the stoichiometry for the FMGT-1:**12** complex was found to be 1:1 with $\text{Log}(K_1) = 9.7\ \text{M}^{-1}$ even though its binding site is identical to **20b**. FMGT-1 was found to be the only FMGT which bound **12** with a stoichiometry different from **21**. The equilibrium constants for complexation between **12** and FMGT-2 and -3 were determined to be $\text{Log}(K_1K_2K_3) = 24.8\ \text{M}^{-3}$ and $\text{Log}(K_1K_2) = 16.2\ \text{M}^{-2}$, respectively. Analogous to this result, it has been reported[26] that Hoechst 33258 binds the hexadecamer **16**, which contains the sequence 5′-AAA TTT-3′ in a 2:1 stoichiometry (this is the only reported instance of Hoechst 33258 binding dsDNA with a stoichiometry greater than 1:1). However, Hoechst 33258 binds to the dodecamer **12b** (CGCAAATTTGCG) with a stoichiometry of 1:1, even though the binding site is identical to that of **16**.[27,29,45,47] It is postulated that the differences in base pairs outside the ligand binding site affect the binding stoichiometry.[45] This may also explain the differences in binding stoichiometries for FMGT-1 with **20** and **12**.

Conclusions

The thermal melting experiments done in this study clearly demonstrate the increased stability of FMGT: dsDNA complexes relative to Hoechst 33258. Less clear is the nature of FMGT binding. It appears likely however that FMGTs bind the A/T rich sequence of **21** in a cooperative manner leading to highly fluorescent complexes. Complexation of **21** outside of the A/T rich sequence likely occurs following saturation of the A/T rich site and leads to non-fluorescent complexes of an unknown motif. Presumably, any higher order complex formed within the A/T rich site occurs through a side-by-side binding motif since there is no other way to fit two or three minor groove binders into a five base pair binding site. Why the parent compound Hoechst 33258 does not also form the higher order complexes is not known although it would have to be assumed that the phenolic hydroxyl plays an important role. Definitive proof of side-by-side binding would require structural investigations which are outside the scope of this study.

The possibility of side-by-side binding is very interesting because of the motifs importance in sequence selective dsDNA recognition. Distamycin and its analogues have been found to bind dsDNA in greater than 1:1 stoichiometries and this knowledge has been used to generate numerous molecules capable of altered sequence selectivity.[4,48–50] A major advance in attempts to obtain active G/C recognition by minor groove binders was the finding that distamycin could form stacked dimers capable of binding to the wider G/C containing minor grooves.[22,51] The possibility that a slight change in Hoechst 33258 leads to higher order binding allows for the incorporation of bisbenzimidazole type moieties in analogous side-by-side binding motifs. In addition to the benefit of fluorescence emission, bisbenzimidazole containing minor groove binders may exhibit better or at least different sequence selectivity compared to their pyrrole peptide counterparts.

The combined equilibrium constant for complexation of two FMGTs can be compared to the equilibrium constant for complexation of one Hoechst 33258 by the same dsDNA by use of eq (7) (derived from ligand: dsDNA equilibrium equations).

$$\frac{[\text{FMGT}-1]^2K_1K_2}{[\text{Ht33258}]K} = \frac{[\text{DNA}:(\text{FMGT}-1)_2]}{[\text{DNA}:\text{Ht33258}]} \qquad (7)$$

At 1 μM unbound ligand concentrations the ratio of [DNA:FMGT-1]/[DNA:Ht33258] would be ~200:1. At nM concentrations the ratio is ~1:1. Replacing [Ht 33258] with [Protein] estimates the ability of FMGTs to inhibit the binding of a protein with a known equilibrium constant (the inhibition of major groove binding proteins may be more complex than shown by eq (7)). Equation (7) predicts that the FMGTs would be more effective inhibitors of protein binding than Hoechst 33258 at concentrations greater than a nM. Studies measuring the ability of FMGTs to inhibit the binding of transcription factors are currently underway.

Experimental

Materials

DNA binding studies. Purified DNA oligomers were purchased from the Biomolecular Resource Center, University of California at San Francisco. Hoechst 33258 and 0.05 wt.% 3-(trimethylsilyl)-propionic-2,2,3,3-d_4 acid, sodium salt in D_2O were bought from Aldrich and used without further purification. Doubly distilled water was used for all solutions.

Organic synthesis. Anhydrous solvents, other solvents, and most reagents were bought from Aldrich Chemical Company and used without further purification. Deuterated solvents were bought from either Aldrich Chemical Company or Cambridge Isotope Laboratories. Some reagents used for solid-phase chemistry including Rink amide MBHA resin, FMOC-Arg(Pbf)-OH, and PyBOP® were bought from Novabiochem and used without further purification. 4-Hydroxybutyrate[37] and 2-

(3-nitro-4-aminophenyl)-6-(4-methyl-1-piperazinyl)-benzimidazole[8] were prepared according to the published methods.

Procedures (ligand:dsDNA experiments)

UV–vis spectroscopy. UV–vis spectra and thermal denaturation experiments were obtained on a Cary 100 Bio UV–vis spectrophotometer equipped with a temperature programmable cell block. All solutions were filtered with a 0.2 μm filter. Constant temperature UV–vis spectra were acquired at 25 °C using a 1 cm path length quartz cuvette and were taken in 0.2% aqueous glacial acetic acid. Molar extinction coefficients were calculated by a single addition of a known quantity of compound (determined by NMR spectroscopy with an internal standard). Due to the previously reported observation that Hoechst 33258 does not obey the Beer–Lambert equation, the concentrations at which each molar extinction coefficient was determined is provided.[30]

Thermal melting experiments were obtained by observing the absorbance of samples at 260 nm while changing the block temperature of the spectrophotometer from 15 to 95 °C in increments of 0.5 °C/min. Sample absorption at 260 nm was between 0.7 and 0.8 at 24 °C in all cases. The melting points of ligand:dsDNA complexes were determined by addition of 3.5 equiv of ligand to a dsDNA sample. All thermal melting experiments were done using 0.01 M potassium phosphate, 0.01 M NaCl, pH 6.9 or 7.2 buffer. All aqueous solutions were mixed with Chelex to remove any trace metal impurities and then filtered. DNA was annealed with its complementary sequence by heating in buffer to 95–99 °C for about 10 min and slowly allowing the solution to cool to room temperature over several hours. Molar extinction coefficients for dsDNA were approximated using $A_{260} = 16800\,M^{-1}$ (G/C basepair)$^{-1}$ and $A_{260} = 13600\,M^{-1}$ (A/T base pair)$^{-1}$; **12** ($A_{260} = 1.9\times10^5$), **20** ($A_{260} = 3.1\times10^5$), **20b** ($A_{260} = 3.1\times10^5$), and **21** ($A_{260} = 3.2\times10^5$). Melting points were determined by first derivative analysis.

Fluorescence spectroscopy. Quantitative determination of the concentrations of the FMGT and Hoechst 33258 solutions were achieved using NMR spectroscopy (Varian Unity Inova 400). An exact volume (usually 100 μL) of 0.05 wt.% 3-(trimethylsilyl)-propionic-2,2,3,3-d_4 acid, sodium salt was added to purified compound dissolved in an exact amount of either D_2O or D_3COD or a mixture of the two solvents. Integration of relative peak intensities of the FMGT and the standard allowed for quantitative determination of both [FMGT] and total number of moles of compound in the NMR sample. Fluorescence spectra were obtained on a Perkin–Elmer LS50B fluorimeter equipped with a constant temperature water bath. All measurements were taken at 24 °C using matched quartz cuvettes. All buffers and solutions used were filtered with a 0.2 μm filter. For all measurements except for those involving **12**, aqueous solutions were mixed with Chelex to remove any trace metal impurities and then filtered after readjusting the pH with dilute aqueous HCl. All measurements were taken in 0.01 M potassium phosphate, 0.01 M NaCl, pH 6.9 or 7.2 buffer unless explicitly stated otherwise. Solutions were mixed by turning the cuvette upside down several times and then allowing the solution to equilibrate for one minute. The solutions were excited at 354 nm. Fluorescence titrations were obtained by titrating a constant concentration of dsDNA, between 1 and 50 nm, with a relatively concentrated solution of ligand, between 0.2 and 40 μM. Emission spectra scanning the region from 400 to 500 nm were taken for each data point. The background fluorescence intensity (buffer and dsDNA) was always subtracted from each data point.

Procedures (organic synthesis)

General. ^{1}H and ^{13}C NMR spectra were obtained on a Varian Unity Inova 400 or 500 spectrometer at 400 MHz and 100 or 150 MHz respectively. TLC was carried out on silica gel (KIESELGER 60 F254) glass backed commercial plates and visualized by UV light. Fast atom bombardment mass spectra, HRMS and LRMS, were obtained on a VG analytical, VG-70E Double Focusing Mass Spectrometer, with an Ion Tech Xenon Gun FAB source, and an OPUS/SIOS data interface and acquisition system. Electrospray ionization mass spectra (ESI) were obtained on a VG Fisons, VG Platform 2, using an ESI source, and a Mass Lynx data acquisition system. Preparative HPLCs were acquired using a Hewlett Packard series 1050 HPLC equipped with a diode array detector. For preparative separations an Alltech Macrosphere 300A, C8, silica, 7 micron, 250×10 mm reverse-phase column was used at 3.0 mL/min solvent flow. Signals were monitored at 260 and 343 nm concurrently. For analytical separations an Alltech Macrosphere 300 RP, C18, 7 micron, 250×4.6 mm column was used at 1.3 mL/min solvent flow in all cases except for FMGT-7 were an Alltech Macrosphere C8, 300A, 7 micron, 250×4.6 mm column was used.

3-(4-Hydroxybutyrate)-benzaldehyde (2). 3-Hydroxybenzaldehyde (1 g, 8.2 mmol), 4-hydroxybutyrate (1.6 g, 8.2 mmol), and triphenyl phosphine (3.4 g, 13.1 mmol) were dissolved in 35 mL anhydrous dichloromethane (DCM) and cooled in an ice bath under an argon atmosphere with stirring. Diethylazodicarboxylate (DEAD) (2.3 g, 13.1 mmol) was slowly added to the reaction vessel by syringe. Reaction progress was monitored by TLC (100% DCM, silica) and stirred for 18 h at room temperature. Solvent was removed by evaporation under reduced pressure and the crude product mixture was purified by flash column chromatography (100% DCM, silica). (942 mg, clear liquid, yield 39%). R_f 0.48 (silica, 100% DCM). ^{1}H NMR ($CDCl_3$) δ 2.17 (m, 2H,-CH_2-), 2.602 (t, 2H, J = 7.2 Hz,-CH_2-C(=O)-), 4.07 (t, 2H, J = 6.1 Hz, Ar-O-CH_2-), 5.15 (s, 2H, Ar-CH_2-), 7.12–7.16 (ArH), 7.34–7.36 (ArH), 7.42–7.46 (ArH), 9.970 (s, 1H,-C(=O)-H) ppm; ^{13}C NMR ($CDCl_3$) δ 19.71 (-C-*C*-C-), 25.95 (-*C*-C(=O)-), 61.60 (Ar-O-*C*-), eleven aromatic signals are detected, 108.02 + 117.077 + 118.72 + 123.49 + 123.5 + 123.80 + 125.27 + 131.07 + 132.99 + 154.57 + 168.10, 187.34 (-*C*(=O)-H) ppm. IR data (ν(cm^{-1})): $\nu_{\text{Aromatic C-H}}$ = 3089 + 3034, $\nu_{\text{Aliphatic C-H}}$ = 2928 + 2847, $\nu_{\text{Aldehydic C-H}}$ = 2730, $\nu_{C=0}$ = 1735 + 1698. LRMS (EI): 192, 177, 164,

105, 91 *m/z*. HRMS (FAB): 299.12829 (calcd 299.128334) $(M+H)^{+1}$ *m/z*.

***meta*-(4-Hydroxybutyrate)-Hoechst, acetate salt (Ht-Ester).** 2-(3-Nitro-4-aminophenyl)-6-(4-methyl-1-piperazinyl)-benzimidazole (154 mg, 0.48 mmol) was hydrogenated according to literature procedure to form the reactive *diortho* amine 2-(3,4-diaminophenyl)-6-(4-methyl-1-piperazinyl)benzimidazole. The *diortho* amine was dried under vacuum for several hours and then without purification added to 10 mL nitrobenzene. To this solution was added 3-(4-hydroxybutyrate)-benzaldehyde (143 mg, 0.48 mmol). The solution was stirred at 140 °C under argon for 24 h.[38] The reaction progress was monitored by TLC (silica, with a gradual addition or triethyl amine and methanol in DCM). When TLC showed the disappearance of most of the 3-(4-hydroxybutyrate)-benzaldehyde, the product was precipitated out with hexanes giving a brownish solid. Successive washes with hexanes removed most residual nitrobenzene. The crude product was then purified by flash chromatrography (silica, ethyl acetate:methanol:triethyamine, 16:8:1). The solid product was collected and then redissolved in methanol and precipitated out of solution with ether. The product was redissolved in dilute aqueous acetic acid and lyopholized. (117 mg, 41%, yellow-brown solid). Pure by analytical HPLC analysis. R_f 0.45 (ethylacetate:-methanol:triethylamine, 16:8:1). ^{1}H NMR (CD_3OD) δ 1.91 (s, acetate), 2.14 (m, 2H,-CH_2-), 2.46 (s, 3H, CH_3N-), 2.60 (t, J = 7.2 Hz, 2H,-CH_2-COR), 2.80 (broad triplet, J = 4.8 Hz, 4H, (-CH_2)$_2$NMe, piperazine), 3.25 (broad triplet, J = 4.5 Hz, 4H, (-$(CH_2)_2$N-Ar, piperazine), 4.11 (t, J = 6.1 Hz, 2H, Ar-O-CH_2-), 5.12 (s, 2H,-CH_2-, benzylic), 7.04 (m, 1H, Ar H), 7.13 (d, J = 2.1 Hz, 1H, Ar H), 7.23–7.33 (m, 3H, Ar H), 7.43 (t, J = 8.3 Hz, 1H, Ar H), 7.50 (d, J = 8.8 Hz, 1H, Ar H), 7.67–7.71 (m, 2H, Ar H), 7.96 (m, 1H, Ar H), 8.27 (bs, 1H, Ar NH) ppm; ^{13}C NMR (CD_3OD) δ 22.89 (Acetate), 26.33 (-*C*-C-C(=O) OH), 32.18 (-C-*C*-C(=O)OH), hidden by solvent peak (Ar-NC-$_2$, piperazine), 56.48 (-C_2NMe, piperazine), 67.82 (-O-C-Ph, benzylic carbon), 68.66 (Ar-O-C-), The following thirteen signals account for all expected unsubstituted aromatic carbon absorptions, 114.13 + 117.06 + 118.84 + 120.82 + 126.56 + 129.70 + 130.02 + 131.89 + 132.34 + 149.92 + 154.23 + 155.61 + 161.46, three low intensity signals possibly due to substituted aromatic carbons were detected at 103.02 + 123.35 + 138.15, 175.21 (acetate), 178.16 (-C(=O)OH) ppm. LRMS (FAB): 601 $(M+H)^{+1}$. HRMS (FAB): 601.293279 (calculated mass = 601.292 714). Analytical HPLC (reverse-phase, C18) 0.1% trifluoroacetic acid (TFA) aqueous with gradient of 0–100% Acetonitrile in 20 min, product eluted at 13.4 min. Fluorescence emission spectrum: broad emission peak centered at 470 nm. UV spectrum: λ_{max} = 255 and 343 nm, λ_{min} = 289 nm, $\epsilon_{343} = 2.8\times10^4$ at $[8.72\times10^{-6}]$.

***meta*-(4-Hydroxybutyric acid)-Hoechst acetate salt (4).** *meta*-(4-Hydroxybutyrate)-Hoechst (515 mg, 0.86 mmol) was dissolved in 15 mL DMF/H_2O (3/1) and excess potassium carbonate was added. The solution was heated with stirring at 110 °C for ~3 h until TLC showed complete disappearance of the ester (silica, ethyl acetate:methanol:triethylamine, 16:8:1). The solvent was removed by evaporation under vacuum to give product plus trace amounts of starting material. 10 mL of 5% aqueous ammonium hydroxide was added to the product mixture which resulted in a colloidal solution. Washing the solution with ethyl acetate resulted in a clear aqueous layer. Drop-wise addition of concentrated HCl to the aqueous layer resulted in precipitation of product upon neutralization of the solution. Solid product was then collected and reconstituted in 0.01 M triethylamine acetate, pH 7 with 30% acetonitrile. The product precipitated out after 24 h at 4 °C as the acetate salt (420 mg, 86%, yellow solid) R_f 0.52 (100% methanol). ^{1}H NMR (DMSO-d_6 + CD_3OD) δ 1.905 (s, acetate), 2.01 (m, 2H,-CH_2-), 2.25 (s, 3H, CH_3-N), 2.42 (t, J = 7.3 Hz, 2H,-CH_2-COR), 3.1–3.2 (broad triplet, 4H, (-CH_2)$_2$NMe, piperazine), 3.8–4.2 (obscured by H-O-D absorption,-(-CH_2)$_2$N-Ar, piperazine), 4.11 (triplet atop H-O-D absorption, J = 6.4 Hz, Ar-O-CH_2-), 6.94 (m, 1H, Ar H), 6.96–7.06 (bs, 1H, Ar H), 7.08 (m, 1H, Ar H), 7.43-7.49 (m, 2H, Ar H), 7.70 (d, J = 8.3 Hz, 1H, Ar H), 8.10–8.12 (m, 2H, Ar H), 8.03 (m, 1H, Ar H), 8.63 (s, 1H, Ar H) ppm; ^{13}C NMR (DMSO-d_6 + CD_3OD) δ 21.24 (Acetate), 24.52 (-*C*-C-C(=O)OH), 30.48 (-C-*C*-C(=O) OH), 45.71 + 45.86 (Ar-NC-$_2$, piperazine), 55.01 (-C_2NMe, piperazine), 67.04 (Ar-O-C-), The following ten signals account for all expected unsubstituted aromatic carbon absorptions, 112.30 + 116.66 + 119.10 + 121.20 + 124.87 + 130.33 + 131.22 + 147.92 + 152.61 + 159.12, 172.26 (acetate), 174.40 (-C(=O)OH) ppm. Mass spectrum (FAB): 511 $(M+H)^{+1}$. HRMS (FAB): 511.245173 (calculated value = 511.245756). Fluorescence emission spectrum: broad emission peak centered at 475 nm. UV spectrum: λ_{max} = 256 and 343 nm, λ_{min} = 287 nm, $\epsilon_{343} = 2.2\times10^4$ at $[7.97\times10^{-6}]$.

FMGT-1. *meta*-(4-Hydroxybutyric acid)-Hoechst acetate salt (**4**) (50 mg, 0.1 mmol) was dissolved in 1 mL dilute HCl(aq) and lyopholized to attain the HCl salt. The yellow powder was then added to tris(2-aminoethyl)amine (190 mg, 1.3 mmol) and PyBOP® (0.15 mmol, 78 mg) in 0.5 mL DMF to give a slightly colloidal solution. The solution was stirred at room temperature for 40 h and the reaction progress monitored by TLC (silica gel using a gradient of concentrated aqueous ammonium hydroxide in methanol). The solution was evaporated under vacuum to give a thick brown oil.

Purification of a fraction of the product mixture was achieved by preparative HPLC reverse-phase chromatography (solvent A = 0.1 M triethylamine acetate, pH 7, solvent B = 100% methanol, solvent C = 0.1% trifluoroacetic acid with 5% acetonitrile). The product was found to elute very slowly with solvent A. Thus, a steep gradient of methanol up to 100% was used in concert with solvent A to remove most impurities. Then the column was flushed with solvent A, then flushed with solvent C, and an increasing gradient of methanol was used in concert with solvent C until the product eluted. Evaporation of solvent gave a thick oil which was dissolved in a methanol/ether mixture and the product was precipitated out with drop wise addition of 12 N HCl and collected by centrifugation to give a bright-yellow solid. Product purity was shown by analytical HPLC.

Quantification of product quantity was achieved by NMR spectroscopy using an internal standard which showed purification of 6.2×10^{6} mol of product as its HCl salt. ^{1}H NMR (D_2O) δ 2.02 (m, 2H,-CH_2-), 2.45 (t, $J=7.34$ Hz, 2H,-CH_2-CONHR), 2.74 (bs, 2H,-C-CH_2-NR_2), 2.90 (bs, 4H,-RN(CH_2-C-N)$_2$), 3.00 (s, CH_3-N-), 3.0-3.1 (m, (-CH_2)$_2$- NMe, piperazine), 3.13 (bs,-RN(C-CH_2-N)$_2$), 3.36 (triplet, $J=6.1$ Hz, 2H, O=C-N-CH_2-), 3.6–3.8 (m, 4H,-(CH_2)$_2$N-Ar, piperazine), 3.82 (bs, 2H, AR-O-CH_2-), integration of all 6 peaks between 6.74 and 7.55 gives 11 protons, this accounts for 1,-(O=C)NH-, and 10, Ar H, protons, 6.74 (bs), 6.90 (bs), 7.07 (broad multiplet), 7.28 (s), 7.41 (bs), 7.55 (broad multiplet) ppm. Fluorescence emission spectrum: broad peak centered at 488 nm. UV spectrum: $\lambda_{max}=255$ and 343 nm, $\lambda_{min}=289$, $\epsilon_{343}=2.2\times10^{4}$ at $[8.95\times10^{-6}]$. LRMS (FAB): 639 $(M+H)^{+1}$. Analytical HPLC (reverse-phase, C18) 0.1% aqueous trifluoroacetic acid (TFA) with gradient of 0–100% acetonitrile in 30 min, product eluted at 11.8 min.

FMGT-2. *meta*-(4-Hydroxybutyric acid)-Hoechst acetate salt (**4**) (10 mg, 0.016 mmol) was dissolved in 1 mL dilute HCl (aq) and lyopholized to attain the HCl salt. The acid was then dissolved in 1 mL DMF with 1.4 equiv PyBOP® (11.4 mg, 0.022 mmol) and 10 equiv spermine (32 mg, 0.16 mmol). TLC (silica, 100% methanol) showed about 50% completion of the reaction, product $R_f\sim0$. The solvent was evaporated under vacuum and the crude reaction mixture redissolved in water. Product was purified by HPLC in the same manner as FMGT-1 and collected as the HCl salt. Product purity was shown by analytical HPLC. Quantification of product quantity was achieved by NMR spectroscopy as for FMGT-1 and showed purification of 6.1×10^{-6} moles of product (yellow solid, yield 38%). ^{1}H NMR (D_2O+D_3COD) δ 1.85 (bs,-N-C-CH_2-CH_2-C-N-), 1.966 (m, Ar-O-C-CH_2-), 2.141 (m, 4H,-N-C-CH_2-C-N-), 2.513 (broad triplet, $J=$ 7.42 Hz, 2H,-CH_2-CONHR), 3.03–3.367 (overlapping signals, protons in β position relative to nonaromatic amines + O=C-N-CH_2-), 3.708 (d, 2H,-(CH_2)$_2$N-Ar, piperazine), 3.906 (d, 2H,-(CH_2)$_2$N-Ar, piperazine), 4.076 (bs, 2H, Ar-O-CH_2-), integration of the aromatic region between 6.9 and 8.2 accounts for all 10 aromatic, Ar H, protons, 7.009 (m), 7.246 (s), 7.291 (m), 7.445 (t, $J=7.98$ Hz), 7.533 (bs), 7.597–7.670 (overlapping signals), 8.114 (s), 8.155 (s) ppm. Fluorescence emission spectrum: broad peak centered at 478 nm. UV spectrum: $\lambda_{max}=256$ and 343, $\lambda_{min}=289$ nm, $\epsilon_{343}=3.5\times10^{4}$ at $[7.56\times10^{-6}]$. LRMS (FAB): 697 $(M+H)^{+1}$. Analytical HPLC (reverse-phase, C18) 0.1% aq TFA with gradient of 0–100% acetonitrile in 20 min, product eluted at 9.4 min.

FMGT-3. The resin-(Arg)$_3$-NH_2 was synthesized using manual FMOC solid-phase techniques with MBHA resin (0.02 mmol loading sites, 50 mg) and 2 equiv of the coupling reagent PyBOP® for each amino acid addition. *meta*-(4-Hydroxybutyric acid)-Hoechst acetate salt (2 equiv, 20 mg, 0.04 mmol) was dissolved in 1 mL dilute HCl (aq) and lyopholized to attain the HCl salt. The 2 equiv of *meta*-(4-hydroxybutyric acid)-Hoechst HCl salt were then added to the deprotected resin with 2 equiv PyBOP® and 4 equiv DIPEA in approximately 2 mL of anhyd DMF. The reaction vessel was very slowly shaken for 20 h and the Kaiser test was negative.

The resin was then thoroughly rinsed with DMF, DCM and MeOH. To cleave the resin and concurrently deprotect the arginine, TFA was added to the reaction vessel along with 2 drops of water and 2 drops of TIS. The reaction vessel was then very slowly shaken for 18 h and the resin beads then filtered from the product/TFA mixture to give a yellow, mildly fluorescent solution. Addition of 8 volumes of ether led to a white precipitate which was separated from the solution by centrifugation. The crude solid was then redissolved in water followed by removal of any undissolved impurities by centrifugation and then lyopholized back to a dry solid. Purification by preparative HPLC and determination of product quantity (through NMR spectroscopy) was achieved in the same manner as for FMGT-1. Product purity was shown by analytical HPLC (yellow solid, 2.1×10^{-6} moles, yield 11%). ^{1}H NMR (D_2O) δ 1.4–1.8 (overlapping signals, 12H,-C-CH_2-CH_2-C-N-, arginine), 2.131 (m, 2H, Ar-O-C-CH_2-), 2.526 (broad triplet, $J=7.0$ Hz, 2H,-CH_2-CONR), 2.9–3.3 (overlapping signals, H_3C-N-(CH_2-)$_2$ + -CH_2-N-C-(N)$_2$), 3.680, 3.708, 3.829, 3.861 (4H,-(CH_2)$_2$N-Ar, piperazine), 4.026 (bs, 2H, Ar-O-CH_2-), 4.15–4.28 (overlapping signals, 3H,-N-CHR-(C=O)-, arginine), integration of the aromatic region between 7.0 and 8.1 accounts for all 10 aromatic, Ar H, protons, 7.028 (bs), 7.190 (s), 7.261, 7.284 (overlapping singlets), 7.391 (bs), 7.476 (broad triplet), 7.554, 7.572 (overlapping singlets), 7.620, 7.642 (overlapping singlets), 7.817 (bs), 8.027 (bs) ppm. Fluorescence emission spectrum: broad peak centered at 478 nm. UV spectrum: $\lambda_{max}=256$ and 343, $\lambda_{min}=289$ nm, $\epsilon_{343}=3.6\times10^{4}$ at $[6.25\times10^{-6}]$. LRMS (ESI): 978 $(M+H)^{+1}$, 488 $(M+2H)^{+2}$. Analytical HPLC (reverse-phase, C18) 0.1% trifluoroacetic acid (TFA) aqueous with gradient of 0–100% acetonitrile in 20 min, product eluted at 9.9 min.

FMGT-5. The resin-(Arg)$_5$-NH_2 was synthesized in the same manner as for FMGT-3 using MBHA resin (0.02 mmol loading sites, 50 mg). Coupling of the deprotected terminal amine of the resin with the Hoechst moiety was also accomplished as for FMGT-3 beginning with *meta*-(4-hydroxybutyric acid)-Hoechst acetate salt (2 equiv, 20 mg, 0.04 mmol). Purification by preparative HPLC and determination of product quantity (through NMR spectroscopy) was achieved in the same manner as for FMGT-1. Product purity was shown by analytical HPLC (yellow solid, 5.1×10^{-6} mol, yield 26%). ^{1}H NMR (D_2O) δ 1.48–1.84 (overlapping signals, 20H,-C-CH_2-CH_2-C-N-, arginine), 2.135 (m, 2H, Ar-O-C-CH_2-), 2.538 (broad triplet, 2H,-CH_2-CONR), 3.001–3.245 (overlapping signals, H_3C-N-(CH_2-)$_2$ + -CH_2-N-C-(N)$_2$), 3.679, 3.707, 3.826, 3.860 (4H,-(CH_2)$_2$N-Ar, piperazine), 4.051 (bs, 2H, Ar-O-CH_2-), 4.233-4.307 (overlapping signals, 5H,-N-CHR-(C=O)-, arginine), integration of the aromatic region between 7.3 and 8.1 accounts for all 10 aromatic, Ar H, protons, 7.038 (bs), 7.188 (s), 7.259, 7.283 (d), 7.415 (bs), 7.493 (bs), 7.563, 7.622, 7.644 (overlapping signals), 7.836 (s), 8.037 (bs) ppm. Fluorescence emission spectrum: broad peak centered at 477 nm. UV spectrum: $\lambda_{max}=256$ and 343, $\lambda_{min}=290$ nm, $\epsilon_{343}=1.74\times10^{4}$ at

[6.60×10^{-6}]. LRMS (ESI): small signal at 1291 $(M+H)^{+1}$, strong signals at 646 and 431 for $(M+2H)^{+2}$ and $(M+3H)^{+3}$, respectively. Analytical HPLC (reverse-phase, C18) 0.1% aqueous trifluoroacetic acid with gradient of 0–100% acetonitrile in 20 min, product eluted at 10.2 min.

Acknowledgement

This work was supported by a grant from the National Institute of Health (5R37DK09171-36).

References and Notes

1. Aymami, J.; Nunn, C. M.; Neidle, S. *Nucl. Acids Res.* **1999**, *27*, 2691.
2. Singh, A. K.; Lown, J. W. *Synth. Commun.* **1998**, *28*, 4059.
3. Bostock-Smith, G. E.; Laughton, C. A.; Searle, M. S. *Nucl. Acids Res.* **1998**, *26*, 1660.
4. Pilch, D. S.; Poklar, N.; Baird, E. E.; Dervan, P. B.; Breslauer, K. J. *Biochemistry* **1999**, *38*, 2143.
5. Pilch, D. S.; Yu, C.; Makhey, D.; LaVoie, E. J.; Srinivasan, A. R.; Olson, W. K.; Sauers, R. R.; Breslauer, K. J.; Geacintov, N. E.; Liu, L. F. *Biochemistry* **1997**, *36*, 12542.
6. Guan, L. L.; Zhao, R. L.; Lown, J. W. *Biochem. Biophys. Res. Commun.* **1997**, *231*, 94.
7. Clark, G. R.; Gray, E. J.; Neidle, S.; Li, Y. H.; Leupin, W. *Biochemistry* **1996**, *35*, 13745–13752.
8. Ebrahimi, S. E. S.; Bibby, M. C.; Fox, K. R.; Douglas, K. T. *Anti-Cancer Drug Des* **1995**, *10*, 463.
9. Parkinson, J. A.; Ebrahimi, S. E.; McKie, J. H.; Douglas, K. T. *Biochemistry* **1994**, *33*, 8442.
10. Bailly, C.; Chaires, J. B. *Bioconjugate Chem.* **1998**, *9*, 513.
11. Geierstanger, B. H.; Wemmer, D. E. *Annu. Rev. Biophys. Biomol. Struct.* **1995**, *24*, 463.
12. Zimmer, C.; Wähnert, U. *Prog. Biophys. Mol. Biol.* **1986**, *47*, 31.
13. Bruice, T. C.; Sengupta, D.; Blasko, A.; Chiang, S. Y.; Beerman, T. A. *Bioorg. Med. Chem.* **1997**, *5*, 685.
14. Bremer, R. E.; Baird, E. E.; Dervan, P. B. *Chem. Biol.* **1998**, *5*, 119.
15. Chiang, S. Y.; Bruice, T. C.; Azizkhan, J. C.; Gawron, L.; Beerman, T. A. *Proc. Natl. Acad. Sci. USA* **1997**, *94*, 2811.
16. Sengupta, D.; Blasko, A.; Bruice, T. C. *Bioorg. Med. Chem.* **1996**, *4*, 803.
17. Bellorini, M.; Moncollin, V.; Dincalci, M.; Mongelli, N.; Mantovani, R. *Nucl. Acids Res.* **1995**, *23*, 1657.
18. Welch, J. J.; Rauscher, F. J.; Beerman, T. A. *J. Biol. Chem.* **1994**, *269*, 31051.
19. Chiang, S. Y.; Welch, J.; Rauscher, F. J.; Beerman, T. A. *Biochemistry* **1994**, *33*, 7033.
20. Dorn, A.; Affolter, M.; Muller, M.; Gehring, W. J.; Leupin, W. *EMBO J.* **1992**, *11*, 279.
21. Dickinson, L. A.; Gulizia, R. J.; Trauger, J. W.; Baird, E. E.; Mosier, D. E.; Gottesfeld, J. M.; Dervan, P. B. *Proc. Natl. Acad. Sci. USA* **1998**, *95*, 12890.
22. Neidle, S. *Biopolymers* **1997**, *44*, 105.
23. Oakley, M. G.; Mrksich, M.; Dervan, P. B. *Biochemistry* **1992**, *31*, 10969.
24. Adnet, F.; Liquier, J.; Taillandier, E.; Singh, M. P.; Rao, K. E.; Lown, J. W. *J. Biomol. Struct. Dyn.* **1992**, *10*, 565.
25. He, G. X.; Browne, K. A.; Blasko, A.; Bruice, T. C. *J. Am. Chem. Soc.* **1994**, *116*, 3716.
26. Browne, K. A.; He, G. X.; Bruice, T. C. *J. Am. Chem. Soc.* **1993**, *115*, 7072.
27. Bostock-Smith, C. E.; Searle, M. S. *Nucl. Acids Res.* **1999**, *27*, 1619.
28. Steinmetzer, K.; Reinert, K. E. *J. Biomol. Struct. Dyn.* **1998**, *15*, 779.
29. Haq, I.; Ladbury, J. E.; Chowdhry, B. Z.; Jenkins, T. C.; Chaires, J. B. *J. Mol. Biol.* **1997**, *271*, 244.
30. Loontiens, F. G.; Regenfuss, P.; Zechel, A.; Dumortier, L.; Clegg, R. M. *Biochemistry* **1990**, *29*, 9029.
31. Harshman, K. D.; Dervan, P. B. *Nucl. Acids Res.* **1985**, *13*, 4825.
32. Loontiens, F. G.; McLaughlin, L. W.; Diekmann, S.; Clegg, R. M. *Biochemistry* **1991**, *30*, 182.
33. Eftink, M. R. *Flouorescence Methods for Studying Equilibrium Macromolecule–Ligand Interactions*; Brand, L., Johnson, M. L., Eds.; Academic: San Diego, 1998; Vol. 278, pp 221–257.
34. Clark, G. R.; Squire, C. J.; Gray, E. J.; Leupin, W.; Neidle, S. *Nucl. Acids Res.* **1996**, *24*, 4882.
35. For a recent investigation of the interactions between DNA and polyarginine, see Mascotti, D. P.; Lohman, T. M. *Biochemistry* **1997**, *36*, 7272.
36. Mitsunobu, O. *Synthesis*, **1981**, 1.
37. Dardoize, F.; Goasdoue, C.; Goasdoue, N.; Laborit, H. M.; Topall, G. *Tetrahedron* **1989**, *45*, 7783.
38. Yadagiri, B.; Lown, J. W. *Synth. Commun.* **1990**, *20*, 955.
39. Coste, J.; Lenguyen, D.; Castro, B. *Tetrahedron Lett.* **1990**, *31*, 205.
40. Kubota, Y. *Bull. Chem. Soc. Jpn* **1990**, *63*, 758.
41. Kubota, Y.; Nakamura, H. *Chem. Lett.*, 745–748.
42. Bailly, C.; Colson, P.; Houssier, C.; Wang, H. Y.; Bathini, Y.; Lown, J. W. *J. Biomol. Struct. Dyn.* **1994**, *12*, 173.
43. Bathini, Y.; Rao, K. E.; Shea, R. G.; Lown, J. W. *Chem. Res. Toxicol.* **1990**, *3*, 268.
44. Robles, J.; McLaughlin, L. W. *J. Am. Chem. Soc.* **1997**, *119*, 6014.
45. Blasko, A.; Bruice, T. C. *Proc. Natl. Acad. Sci. USA* **1993**, *90*, 10018.
46. The equilibrium association constant and stoichiometry for the complexation of dsDNA **12** by Hoechst 33258 has been previously reported by Loontiens et al. (ref 32) to be $\mathrm{Log(K)} = 8.5\,\mathrm{M}^{-1}$ and 1:1.
47. The equilibrium association constant for the binding of Hoechst 33258 to **12b** was determined to be $\mathrm{Log(K)} = 8.5\,\mathrm{M}^{-1}$ (ref 29).
48. de Clairac, R. P. L.; Seel, C. J.; Geierstanger, B. H.; Mrksich, M.; Baird, E. E.; Dervan, P. B.; Wemmer, D. E. *J. Am. Chem. Soc.* **1999**, *121*, 2956.
49. Herman, D. M.; Turner, J. M.; Baird, E. E.; Dervan, P. B. *J. Am. Chem. Soc.* **1999**, *121*, 1121.
50. Swalley, S. E.; Baird, E. E.; Dervan, P. B. *J. Am. Chem. Soc.* **1999**, *121*, 1113.
51. Kopka, M. L.; Goodsell, D. S.; Han, G. W.; Chiu, T. K.; Lown, J. W.; Dickerson, R. E. *Structure* **1997**, *5*, 1033.